PHYSICAL REVIEW B **84**, 165405 (2011)

Ionization in organic thin films: Electrostatic potential, electronic polarization, and dopants in pentacene films

Benjamin J. Topham and Zoltán G. Soos*
Department of Chemistry, Princeton University, Princeton New Jersey 08544, USA
(Received 14 July 2011; published 4 October 2011)

Ionization processes in thin films are central to organic electronics. The ionization potential $I(p)$ or electron affinity $A(p)$ of any molecule p depends on the electronic polarization of the surrounding molecules and on electrostatic interactions $W(p)$ that are evaluated in films using the potential $\Phi^{(g)}(\mathbf{r})$ due to gas-phase charge densities. $W(p)$ is combined with a self-consistent treatment of electronic polarization to obtain $I(p)$ and $A(p)$ using molecular quantum theory and the film's structure. $I(p)$ and $A(p)$ are not additive but contain cross terms in electronic polarization and electrostatics. The procedure accounts quantitatively for $I(p)$ of pentacene and perfluoropentacene films with standing molecules in bilayers or lying molecules in monolayers. Surface or subsurface dopants in pentacene films are modeled as ion pairs with Coulomb interactions between a fixed anion and an adjacent cation. Variations of $\Phi^{(g)}(\mathbf{r})$ due to an ion pair modulate $I(p)$ and $A(p)$ locally and rationalize observed changes for tunneling into occupied and unoccupied pentacene states, respectively. As in molecular exciton theory, intermolecular overlap is neglected in the computation of $I(p)$ or $A(p)$. Electrostatic interactions are conveniently quantified by $\Phi^{(g)}(0)$ at the center of molecules.

DOI: 10.1103/PhysRevB.84.165405 PACS number(s): 77.22.−d, 73.20.−r, 79.60.Dp, 81.05.Fb

I. INTRODUCTION

Research in organic electronics[1–4] has focused on devices such as light-emitting diodes, thin-film transistors, and solar cells based on conjugated molecules or polymers. Weak nonspecific bonding facilitates the formation of interfaces while thin films compensate for the limited mobility of charges in organic solids. Much progress can be attributed to the preparation and characterization of thin films.[5] Charge injection and extraction from electrodes are fundamental to device operation. Hole injection into the highest occupied molecular orbital (HOMO) is characterized by ultraviolet photoelectron spectroscopy (UPS), x-ray photoelectron spectroscopy (XPS), or scanning tunneling spectroscopy (STS). The barrier to hole injection is I-E_F in the Schottky-Mott limit, where I is the ionization potential at the surface and E_F is the Fermi energy of the metal. Electron injection into the lowest unoccupied molecular orbital (MO) is studied by inverse photoelectron spectroscopy (IPES) or STS. The barrier for electron injection is E_F-A, where A is the electron affinity at the surface. In either case, due to limited intermolecular overlap, a localized or nearly localized charge is generated in organic thin films that are extended in two dimensions and finite in the third. Molecular energy levels are of central importance even though metal-organic interfaces typically deviate[3,4] from the Schottky-Mott limit. Our treatment of ionization in thin organic films focuses on Coulomb interactions between molecules with delocalized MOs.

Two recent studies highlighted ionization processes. Saltzmann *et al.*[6] reported UPS spectra of pentacene and perfluoropentacene films in which molecules were either lying down or standing up, as well as mixed films of variable composition. Ionization potentials can clearly be tuned by molecular orientation and film composition, and the observed trends follow from molecular electrostatics.[7] We model these spectra quantitatively by combining the electrostatic potential $\Phi^{(g)}(\mathbf{r})$ of molecules with electronic polarization in films. Ha and Kahn[8,9] applied scanning tunneling microscopy (STM) to pentacene films with surface or subsurface dopants. Bright and dark spots for tunneling into occupied pentacene states indicate lower and higher ionization potentials, respectively, while bright spots for tunneling into unoccupied states indicate higher electron affinity. STM probes local changes that we analyze in terms of $\Phi^{(g)}(\mathbf{r})$. Both studies identify changes of I or A under conditions that bring out electrostatic contributions related to $\Phi^{(g)}(\mathbf{r})$.

An oriented gas is the starting point of molecular exciton theory for organic crystals. Van der Waals or weak intermolecular interactions are taken as perturbations of isolated (gas phase) molecules. The theory describes the gas-to-crystal shift of electronic excitations and their splitting into Davydov components when the unit cell contains several molecules. An oriented gas is a well defined limit of no intermolecular interactions or overlap and strictly localized electronic excitations. It is accessible to quantum chemistry since molecular properties, mainly ground state properties, are required. Van der Waals interactions in solids, on the other hand, are still difficult for density functional theory (DFT) and extended systems with interfaces present major computational challenges. In this paper, we combine DFT for molecules with crystal or film structure to compute ionization potentials and electron affinities in organic thin films. Ionization in films is a new application of the theory, distinct from singlet or triplet excitons in crystals.

We consider molecular films, which are better characterized structurally, but the analysis holds with some modifications for polymer films. The ionization potential $I(p)$ and electron affinity $A(p)$ of molecule p in a film are related to the gas phase as

$$\begin{aligned} I(p) &= I_g - P_+(p), \\ A(p) &= A_g + P_-(p). \end{aligned} \tag{1}$$

By longstanding convention,[10,11] the polarization energy $P(p)$ includes everything: electrostatics, electronic

 ©2011 American Physical Society

polarization, and molecular and lattice relaxation. Molecular and lattice relaxation are 5–10% corrections, as discussed by Silinsh and Capek,[12] that we neglect. Electronic polarization is the only contribution in systems of neutral atoms. Neutral molecules also have electrostatic contributions $W(p)$ that are related to molecular shape[13] and that correspond to charge-quadrupole interactions in systems of nonpolar molecules. Hence Bounds and Munn[14] referred to $P(p)$ in Eq. (1) as the "apparent polarization." The definition of polarization relative to the gas phase is a thought experiment in which a molecular ion is generated in an infinite crystal. The position dependence of $P(p)$ follows immediately in a film or a finite crystal. Other considerations such as Fermi level shifts or electron inelastic mean free paths enter in thin film spectra from which $P(p)$, typically $P_+(p)$, can be extracted.

The ionization of molecule p in an oriented gas changes the local charge distribution. The change $\Delta\rho$ is coupled to the electrostatic potential $\Phi^{(g)}$ of all other molecules,[15] which introduces the structure of the gas. The electrostatic energy is[15]

$$W(p) = -\int d^3\vec{r}\,\Delta\rho_{\pm}^{(g)}(\vec{r})\Phi^{(g)}(\vec{r}),$$
$$\Delta\rho_{\pm}^{(g)}(\vec{r}) = \rho_{\pm}^{(g)}(\vec{r}) - \rho_{p}^{(g)}(\vec{r}). \tag{2}$$

Here superscripts refer to the gas phase: $\rho^{(g)}(\mathbf{r})$ is the ground state charge density (in units of e) of the molecule or molecular ion. In exciton theory, $W(p)$ corresponds to the $I(p)$ or $A(p)$ shift in an oriented gas of unpolarized molecules. We recover $W(p)$ in Sec. II from a general treatment of $I(p)$ that also includes electronic polarization. $W(p)$ can readily be evaluated for different molecular arrangements. Positive $\Phi^{(g)}$ raises the energy of the cation and hence increases $I(p)$, while it stabilizes the anion and hence increases $A(p)$. A convenient quantitative measure of the potential is its value $\Phi^{(g)}(0)$ at the center of any molecule.

Electronic polarization is charge redistribution from $\rho^{(g)}(\mathbf{r})$ to $\rho(\mathbf{r})$ in the film. The relevant molecular property is the polarizability tensor α. In classical physics, the Clausius-Mosotti equation relates the dielectric constant in a gas or solution to the scalar α of atoms or the trace of α for nonpolar molecules, while the Debye equation is the generalization to polar molecules. Mott and Littleton[16] first treated atomic lattices as polarizable points. Microelectrostatics[12,17] is the extension to molecular crystals with multiple polarizable points per conjugated molecule. Charge redistribution in a potential is strictly intramolecular in the absence of overlap. In this limit we have classical Coulomb interactions between quantum mechanical molecules or ions.[18] Electronic contributions to $P(p)$ in Eq. (1) depend on α as well as $W(p)$ and there are cross terms between polarization and electrostatics.[13,18] In the absence of overlap, $I(p)$ and $A(p)$ in Eq. (1) can be estimated for given molecular arrangements using only quantum mechanics of isolated molecules.

The paper is organized as follows. The general development of $I(p)$ or $A(p)$ in Sec. II presents the approximations under which we calculate $P(p)$ in films and explicitly identifies electrostatic and polarization contributions. In Sec. III we obtain $I(p)$ in pentacene and perfluoropentacene films to model the UPS spectra of Saltzmann *et al.*.[6] Molecular inputs and film structure are quantitative at the present resolution. We relate $W(p)$ in Sec. IV to $I(p)$ and $A(p)$ changes in pentacene films with electronic dopants that are modeled as a fixed dopant anion and an adjacent pentacene cation. Bright and dark STM images are related to the electrostatic potentials $\Phi^{(g)}$ of ion pairs on the surface or below the surface, with the polarity of the tip controlling the cation's location on the surface. Section V briefly summarizes the roles of electrostatics and electronic polarization in organic thin films.

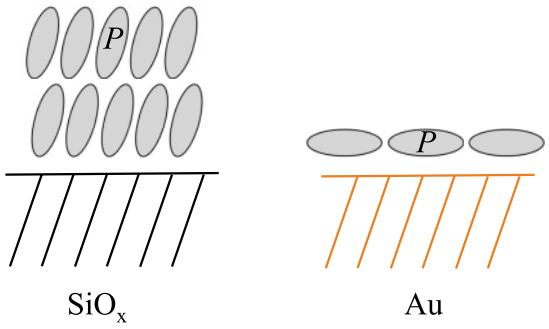

FIG. 1. (Color online) Schematic representation of films of standing pentacene (P) molecules on SiO_x and lying P on Au(111).

II. IONIZATION IN ORGANIC THIN FILMS

We model a film by a fixed array $\{a\}$ of molecules or molecular ions with electrostatic energy $E_0(\{a\})$ as sketched in Fig. 1 for films discussed in Sec. III. $E_0(\{a\})$ is an intermolecular quantity that vanishes when molecules are infinitely far apart. It depends on the charge distribution of $\{a\}$ but not I or A for producing ions. The ionization of molecule p gives an array $\{a,p\}$ with electrostatic energy $E_0 + P_+(p)$, where $P_+(p)$ is limited to electronic contributions. Similarly, an array with a negative ion at p has electrostatic energy $E_0 + P_-(p)$. Neutral molecules have gas-phase charge density $\rho^{(g)}(\mathbf{r})$ while isolated ions have charge density $\rho_+^{(g)}(\mathbf{r})$ or $\rho_-^{(g)}(\mathbf{r})$. The location of molecules and ions in the array is indicated below by subscripts. We consider gas-phase charges to be fixed sources that generate an electrostatic potential $\Phi^{(g)}(\mathbf{r})$ in the array $\{a\}$. The electrostatic energy of the oriented gas is based on gas phase potentials and charge densities.

To include polarization, we treat molecules or ions in $\{a\}$ as polarizable quantum mechanical objects. $E_0(\{a\})$ is minimized by charge densities, to be determined, $\rho_a(\mathbf{r}) - \rho_a^{(g)}(\mathbf{r}) = \delta\rho_a(\mathbf{r})$ that depend on the array's structure.[18] $E_0 + P_+(p)$ has additional charge redistribution due to the cation. In general, $P_+(p)$ or $P_-(p)$ is the difference between two extensive quantities,[18] an array in which site p is ionized and another array in which site p is neutral.

Gas-phase charges generate $\Phi_a^{(g)}(\mathbf{r})$ in the array $\{a\}$ while redistributed charges generate potentials $\phi_a(\mathbf{r})$. The electrostatic energy of the array is[13,18]

$$E_0(\{a\}) = \frac{1}{2}\sum_a \langle\rho_a^{(g)}|\phi_a\rangle = \frac{1}{2}\sum_a \langle\rho_a|\Phi_a^{(g)}\rangle, \tag{3}$$

where

$$\langle \rho_a^{(g)} | \phi_a \rangle \equiv \int_V d^3\vec{r}\, \rho_a^{(g)}(\vec{r})\phi_a(\vec{r}),$$
$$\phi_a(\vec{r}) = \sum_{b,b\neq a} \int_{V_b} d^3\vec{r}'\, \rho_b(\vec{r}')/|\vec{r}' - \vec{r}|. \tag{4}$$

The two expressions in Eq. (3) are equal since the Coulomb interaction is bilinear in charge. An ion at site p produces additional charge redistribution. Gas-phase charges in $\{a,p\}$ are the same except at $a = p$. A cation at p leads to

$$\rho_{a,p}^{(g)} = \rho_a^{(g)} + \Delta\rho_p^{(g)}\delta_{ap}, \tag{5}$$

where $\Delta\rho_p^{(g)}$ is given in Eq. (2). The potentials $\Phi_a^{(g)}(\mathbf{r})$ change everywhere except at $a = p$. The energy difference $E_0(\{a,p\}) - E_0(\{a\})$ is obtained with the aid of Eq. (5),

$$P_+(p) = -\frac{1}{2}\langle \Delta\rho_p^{(g)} | \Delta\phi_p \rangle - \frac{1}{2}\langle \Delta\rho_p^{(g)} | \Phi_p^{(g)} \rangle - \frac{1}{2}\sum_a \langle \rho_a^{(g)} | \phi_{a,p} - \phi_a \rangle. \tag{6}$$

The second term is $W(p)/2$ in Eq. (2). Using Eq. (3), we change the sum in Eq. (6) to integrals over $\Phi_a^{(g)}$ and redistributed charges in the two arrays. The $a = p$ term is $W(p)/2$ plus charge redistribution at p. The final expression for $P_+(p)$ is

$$P_+(p) = -\frac{1}{2}\langle \Delta\rho_p^{(g)} | \Delta\phi_p \rangle + W(p) - \frac{1}{2}\sum_a \langle \delta\rho_{a,p} | \Phi_a^{(g)} \rangle. \tag{7}$$

Here $\delta\rho_{a,p}(\mathbf{r}) = \rho_a(\mathbf{r}) - \rho_a^{(g)}(\mathbf{r})$ is charge redistribution at sites $a \neq p$, while $\delta\rho_{p,p}(\mathbf{r}) = \delta\rho_+^{(g)}(\mathbf{r}) - \delta\rho_p^{(g)}(\mathbf{r})$ is the difference of the polarization of the cation and neutral molecule. Equation (7) is identical to Eq. (3) of Ref. 13. We have rearranged sums to bring out the physical origin of various contributions.

To first order in Coulomb interactions, $E_0^{(1)}(\{a\})$ has gas-phase charges everywhere in Eq. (3). It follows immediately that

$$W(p) = E_0^{(1)}(\{a,p\}) - E_0^{(1)}(\{a\}). \tag{8}$$

$W(p)$ in Eqs. (2) or (8) corresponds to charge-multipole interactions when $\{a\}$ is an array of neutral molecules. Gauss' theorem gives $W(p) = 0$ for neutral atoms with spherically symmetric $\rho^{(g)}(\mathbf{r})$. We also consider arrays with ions at other sites than p, when $W(p)$ contains Coulomb interactions between ions as well as charge-multipole interactions. We can view $W(p)$ in Eq. (2) as a localized charge distribution $\Delta\rho^{(g)}(\mathbf{r})$ in an external potential $\Phi^{(g)}(\mathbf{r})$. Multipole expansion[15] of $\Delta\rho^{(g)}(\mathbf{r})$ gives a net charge $|e|$, no dipole $\mathbf{p}$ when the molecule has inversion symmetry, quadrupole moments $\mathcal{Q}_{ij}$ for $i,j = x,y,z$, and so on. The leading term is $W(p) \sim -e\Phi^{(g)}(0)$, the potential at the center of the molecule. This simple approximation can be compared to the integral in Eq. (2), and $\Phi^{(g)}(0)$ turns out to be a convenient way to quantify the potential at every molecule.

We define the first term of Eq. (7) as $E_P(p)$ for electronic polarization since $\Delta\phi_p$ is entirely due to charge redistribution because $\Phi_p^{(g)}(\mathbf{r})$ does not change at site p. $E_P(p)$ always stabilizes the ion, thereby decreasing $I(p)$ and increasing $A(p)$ in Eq. (1). Mott and Littleton[12] estimated $E_P(p)$ for an atomic lattice. Fully self-consistent $E_P(p)$ are currently used to analyze UPS spectra of noble gas clusters[19,20] with calculated or measured atomic polarizabilities α. As discussed by Fox,[21] Munn,[17,22] Silinsh,[12] and others, similar $E_P(p)$ calculations can be performed self-consistently on naphthalene, anthracene, or other conjugated molecules by partitioning α among rings or heavy atoms, although the dependence on the partitioning is unsatisfactory. The last term of Eq. (7) corresponds to electrostatic interactions of redistributed charges with the gas-phase potentials of $\{a\}$. Mixed terms follow directly from the general expression for E_0 in Eq. (3) and indicate that $P(p)$ is not simply additive in molecular systems.

Aside from the approximation of no overlap, the development is general and holds for arrays of different molecules and/or molecular ions. In practice, we require crystalline arrays with a specified structure to compute potentials efficiently and a method that relates charge redistribution to potentials. Zero overlap limits $\delta\rho(\mathbf{r})$ to molecules and is formally given by the functional derivative $\delta\rho(\mathbf{r})/\delta\Phi(\mathbf{r}')$ with $\mathbf{r}$, $\mathbf{r}'$ in the same molecule or ion. As recognized by Tsiper and Soos,[18] the calculation of $E_P(p)$ becomes practical when the continuous distribution $\rho(\mathbf{r})$ is replaced by partial charges ρ_m at atom m and changes of ρ_m are obtained using a semi-empirical Hamiltonian in which the atomic potential is a diagonal site energy. To be self-consistent, the same H must be used for both atomic charges $\rho_m^{(g)}$ and the resulting potentials $\phi_m^{(g)}$ that differ from the best available $\Phi^{(g)}(\mathbf{r}_m)$. The symmetric tensor Π_{nm} that describes atom-atom polarizability is[18]

$$\Pi_{\mathrm{nm}} = -\left(\frac{\partial\rho_n}{\partial\phi_m}\right)_0 = -\left(\frac{\partial\rho_m}{\partial\phi_n}\right)_0 = -\left(\frac{\partial^2\epsilon_0}{\partial\phi_m\partial\phi_n}\right)_0 \tag{9}$$

for atoms n, m of a molecule or ion with ground state energy ϵ_0. Charge redistribution within the array is then governed by

$$\rho_n = \rho_n^{(g)} - \sum_m \Pi_{\mathrm{nm}}\phi_m, \tag{10}$$

where $\rho_n^{(g)}$ is the gas-phase atomic charge associated with $\rho^{(g)}(\mathbf{r})$. We compute Π_{nm} for the gas-phase ground state using intermediate neglect of differential overlap/spectroscopy (INDO/S)[23] and solve Eq. (10) iteratively starting with gas-phase potentials $\phi_m^{(g)}$. We also include[18] induced atomic dipoles $\delta\mu_{\mathrm{m}}$ to reproduce the best available gas-phase polarizability tensor α, either measured or calculated. Induced dipoles contribute to ϕ_m. We monitor Π_{nm} as charges redistribute,[18,24] but presumably due to weak intermolecular interactions, have not found it necessary to recalculate the tensor in systems studied to date.

The combination of discrete atomic charges and induced atomic dipoles with INDO/S provides a self-consistent way to compute $E_P(p)$, the first term in Eq. (7). The present development shows that $W(p)$ can be evaluated independently with any gas-phase potential $\Phi^{(g)}$. We also use $\Phi^{(g)}$ in the cross

term. The discrete version of Eq. (7) is

$$P_+(p) = -\frac{1}{2}\sum_{m\in p}\Delta\rho_m^{(g)}\Delta\phi_m - \sum_{m\in p}\Delta\rho_m^{(g)}\Phi_m^{(g)} - \frac{1}{2}\sum_a\sum_j\left(\delta\rho_j^a\Phi_j^{a(g)} - \delta\vec{\mu}_j^a\cdot\vec{F}_j^{a(g)}\right), \qquad (11)$$

where $\mathbf{F}^{(g)} = -\nabla\Phi^{(g)}$ is the electric field of the gas-phase potential evaluated at atoms. The first two sums are over the atoms of molecule p, while the third sum is over atoms j of all molecules $\{a\}$. Equation (11) is identical to Eq. (27) of Ref. 18 aside from replacing the INDO/S potential by $\Phi^{(g)}$. We evaluate $\Phi^{(g)}(\mathbf{r}_m)$ at atom m of molecule p using gas-phase $\rho^{(g)}(\mathbf{r}')$ in Eq. (4). The same sum is generated in a film of neutral molecules by the potential of molecule p at atom m of all other molecules.[25] Potentials outside a localized charge distribution are routinely evaluated in quantum chemistry codes. They are summed over atomic positions $\mathbf{r}_m$ that are related by lattice vectors.

Coulomb interactions are long ranged. The leading term of $W(p) = -e\Phi^{(g)}(0)$ goes as r^{-3} for a neutral array $\{a\}$ with charge-quadrupole interactions. The volume integral of $W(p)$ goes as dr/r and has a logarithmic divergence at large r. Hence $I(p)$ or $A(p)$ depends on the macroscopic shape of the sample. Other contributions to $P(p)$ in Eq. (7) converge more rapidly and do not depend on the macroscopic shape. The transport gap,[26] $I(p) - A(p)$, has the combination $P_+(p) + P_-(p)$ that converges[18] as $1/R$, where R is the radius of a sphere centered on p and charge redistribution of all molecules in the sphere is included. Thin films are extended in two dimensions. Now $W(p)$ converges as $1/R$ and $I(p)$ or $A(p)$ is well defined separately.[13] To compute $P(p)$ in Eq. (11), we consider[27] a pill box with the origin at the center of molecule p. The film's thickness d defines the height d or $2d$ of the box for an insulating or metallic substrate, respectively. The radius R is progressively increased and $P(p,R)$ is evaluated using all molecules in the pill box. Up to 10^4 molecules with 30–50 atoms each are routinely included.[28] The evolution of $\Phi^{(g)}(0)$ with R is shown in Fig. 2 for films studied in Sec. III, two standing bilayers of pentacene on SiO_x and two lying monolayers on Au(1,1,1) whose image charge gives a dipole with faster convergence. After confirming the $1/R$ dependence, we extrapolate to find $\Phi^{(g)}(0)$. The full calculation of $W(p)$ in Eq. (11) has extrapolated $\Phi^{(g)}(\mathbf{r}_m)$ at all atoms.

Results for $\Phi^{(g)}$ in Eq. (11) and for I_g or A_g in Eq. (1) are based on the Becke three-parameter Lee-Yang-Parr (B3LYP) potential with the 6-311^{++}G** basis in the GAUSSIAN 03 program.[29] The self-consistent calculation of Eq. (11) is performed using INDO/S.[23] The second and third sums are then computed again using $\Phi^{(g)}$. Hence $P(p)$ is evaluated with both potentials. The differences are typically small and related to atomic charges.[28] For example, Hückel theory has $\rho_m = 0$ and hence $W(p) = 0$ for alternant hydrocarbons such as pentacene or perfluoropentacene. INDO/S has small ρ_m for pentacene, large ρ_m for perfluoropentacene. The B3LYP potential is clearly preferable.

We conclude the general treatment of $P(p)$ with a comment about approximations. The electrostatic energy $W(p)$ in Eq. (2) rigorously gives gas-to-film shifts for molecules with $\alpha = 0$.

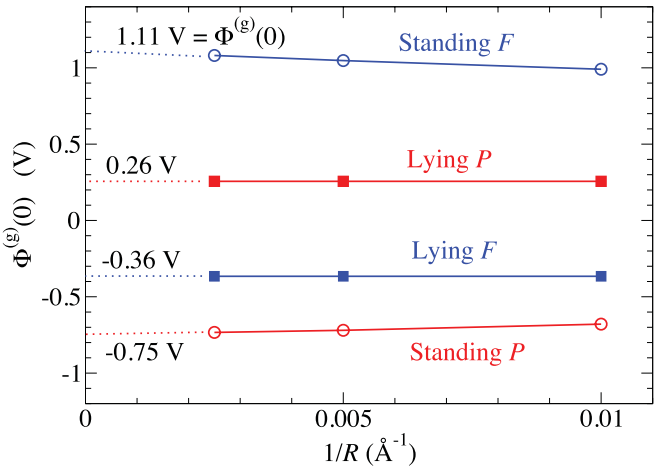

FIG. 2. (Color online) Calculated electrostatic potential $\Phi^{(g)}(0)$ at the center of a pentacene (P) or perfluoropentacene (F) molecule at the center a pillbox of radius R (Å). Standing films are bilayers on SiO_x; lying films are monolayers on Au(111).

When polarizability is considered, however, $P(p)$ does not separate into electrostatics and polarization since there are cross terms. Consistency requires using the same Hamiltonian for $P(p)$. The compromise of INDO/S for charge redistribution in $E_P(p)$ and B3LYP for electrostatics is not self consistent. It represents first-order corrections[25] to self-consistent INDO/S results in the difference between gas-phase B3LYP and INDO/S potentials.

III. PENTACENE AND PERFLUOROPENTACENE FILMS

As sketched in Fig. 1, pentacene (P) or perfluoropentacene (F) films on SiO_x have standing molecules that closely approximate an ab layer of the crystal. Monolayers on Au(1,1,1) instead have lying down molecules. The P/F composition can be varied in films on SiO_x. There are also films with intermediate orientation.[30] As discussed in a series of papers,[6,30] UPS spectra in Fig. 3 probe the dependence of $I(p)$ on orientation and composition, and molecular electrostatics[7] accounts for the observed trends of binding energy (BE) in terms of the polarity of C-H and C-F bonds. $I(p)$ is the peak with the lowest BE. There are several sources of broadening whose relative magnitudes are poorly understood at present.[4] In addition to instrumental resolution, they include the ionization of subsurface molecules governed by the electron inelastic scattering length, structural disorder, vibrationally excited final states, and delocalization or band formation due to overlap. Comparison of BE or $I(p)$ is limited to about ± 0.2 eV, which, however, is a major advance over initial estimates of $I(p)$ in organic crystals.[10,11] The bars in Fig. 3 are calculated $I(p)$ as described below that agree remarkably well with experiment.

The gas-to-film shift of $I(p)$ is given by $P_+(p)$ in Eq. (11), which contains all variations of $I(p)$ with molecular orientation or film thickness. The π systems of P and F are nominally identical. Table I contains B3LYP results with the 6-311^{++}G** basis. The vertical ionization potential I_g and electron affinity A_g agree fairly well with experiment.[31,32]

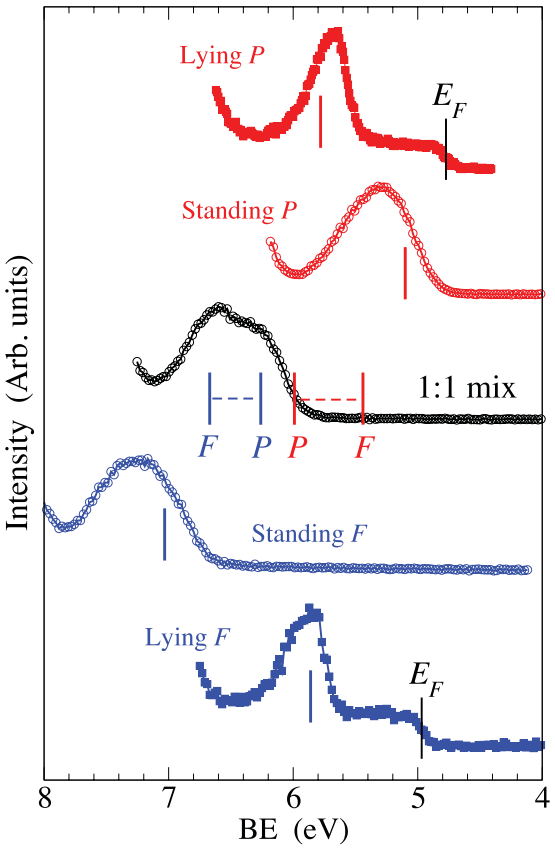

FIG. 3. (Color online) Calculated (bars) and measured (Ref. 6) photoelectron spectra of pentacene (P) and perfluoropentacene (F) films, standing bilayers on SiO_x and lying monolayers on Au(111). The calculated binding energy of P and F in the 1:1 mixed bilayer is for two hypothetical structures discussed in the text.

As expected, the π systems have similar α tensors. The tensor has large components in the molecular plane and its principal axes are fixed by symmetry. The INDO/S results in parentheses work well in the plane and thus account for most of the polarizability, but not for the small out-of-plane component that requires a larger basis. Induced atomic dipoles are introduced in the self-consistent calculation[18] to reproduce the B3LYP α. The atom-atom polarizability tensor Π in Eq. (9) has dimension 36 for P ($C_{22}H_{14}$) or F ($C_{22}F_{14}$). The largest elements are diagonal for C atoms and off diagonal for nearby C atoms. These elements differ by less than 5%. Table I also contains the principal components of the calculated quadrupole tensor $\mathcal{Q}$. The components of this traceless tensor have opposite signs for P and F, consistent with the polarity of C-H and C-F bonds. Multipole expansions are not useful when molecular dimensions exceed intermolecular separations. We calculate $\Phi^{(g)}(\mathbf{r})$ directly from $\rho^{(g)}(\mathbf{r})$, thereby implicitly including all multipoles. The tensors α and $\mathcal{Q}$ illustrate the similar polarizability and opposite electrostatics of P and F.

To start with pure films in Fig. 3, we consider ab layers from the bulk[33] P or[34] F crystals for films of standing molecules on SiO_x. The layer thickness of 1.5 nm is large enough to neglect the insulating substrate. $P_+(p)$ of a bilayer is almost independent of additional ab layers.[13] The four molecules per

TABLE I. DFT molecular inputs for pentacene (P) and perfluoropentacene (F).

	P	F
I_g (eV)	6.46 (6.6)[a]	7.24 (7.5)[a]
A_g (eV)	1.52	2.68
α_{XX} (Å^3)	99.48 (89.47)[b]	96.86 (94.85)[b]
α_{YY} (Å^3)	38.02 (39.40)	41.30 (43.22)
α_{ZZ} (Å^3)	18.02 (0.06)	17.09 (0.02)
$\mathcal{Q}_{XX}$ (DÅ)	8.78	−11.40
$\mathcal{Q}_{YY}$ (DÅ)	8.47	−12.16
$\mathcal{Q}_{ZZ}$ (DÅ)	−17.25	23.56

[a]Experiment from Refs. 31 and 32.
[b]INDO/S.

pentacene unit cell come in two nearly equivalent pairs. We use pair I of Ref. 24 and two molecules per unit cell for standing bilayers, and the monolayer structure[35] of lying P or F on Au(1,1,1). We approximate Au(1,1,1) by a constant potential surface with image charges and image dipoles.[27] The molecular plane is taken at be 0.4 nm from the metal. Calculated $I(p) = I_g - P_+(p)$ are listed in Table II and shown in Fig. 3. The measured and calculated $I(p)$ of P and F films are fully consistent.

Turning to $P_+(p)$ contributions in Table II, we see that electronic polarization is $E_P(p) \sim 1$ eV and depends weakly on orientation. The third and last columns are $W(p)$ and the cross term, respectively. Either standing vs. lying or C-F vs. C-H bonds changes the sign of $W(p)$, which consequently governs the direction of the shifts in Fig. 3 as has already been discussed[7] in detail for dipoles and quadrupoles of C-F bonds and π clouds. Saltzmann *et al.*[6] reported binding energy shifts from the red edge of the UPS spectrum: −0.55 eV between standing and lying P and 0.85 eV between standing and lying F. The corresponding $I(p)$ changes in Table II are −0.68 and 1.17 eV. By itself, the electrostatic contribution $W(p)$ overestimates the shifts as −0.97 and 1.39 eV.

The spectrum of a standing 1:1 P/F bilayer in Fig. 3 shows two partly resolved peaks at intermediate BE. Similar spectra of standing 3:1 or 1:3 P/F bilayers again show intermediate BE.[6,7] Structures are not available for films with variable composition. An idealized structure of a 1:1 ab layer of standing P and F can be estimated by energy minimization, but we chose instead to explore variations of $I(p)$ in hypothetical 1:1 films. The limiting cases are an ab layer of P with one sublattice replaced by F and an ab layer of F with

TABLE II. $I(p)$ (in eV) and contributions to $P_+(p)$ [Eq. (11), in eV]. $E_P(p)$ is electronic polarization and $W(p)$ is electrostatics.

Film	$I(p)$	$E_P(p)$	$W(p)$	cross terms
P (standing)	5.10	1.03	0.78	0.35
F (standing)	7.03	1.40	−1.05	0.05
P (lying)	5.78	0.84	−0.29	0.13
F (lying)	5.86	0.80	0.39	0.18
P(1:1)[a]	5.99/5.44	1.22/1.20	−0.32/−0.04	−0.39/0.24
F(1:1)[a]	6.26/6.67	1.24/1.12	−0.03/−0.32	−0.23/−0.23

[a]The first/second entry is for the standing P/F structure.

one sublattice replaced by P. In effect H and F atoms are interchanged in the carbon cores. The P structure leads to similar $I(p)$ in Table II for the 1:1 film while the F structure substantially increases $I(p)$ of F from 6.26 to 6.67 eV and decreases $I(p)$ of P from 5.99 to 5.44 eV.

The surprisingly large range of $I(p)$ in the limiting 1:1 structures are shown in Fig. 3. To eliminate the range, we equalize the structures in steps. The unit cell volumes are $V_c =$ 692 Å^3 for[33] P and 797 Å^3 for[34] F. We expand (compress) the P (F) unit cells uniformly to the average V_c. The $I(p)$ range decreases slightly, but equalizing V_c is a small correction. Next we use the mean orientation of P and F in structures with equal V_c. Orientation is also a small correction. It turns out that $I(p)$ is sensitive to the herringbone packing. The ab layer of P discussed in Sec. IV and shown in Fig. 5 has nearest neighbors in opposite sublattices while the ab layer of F has nearest neighbors in the same sublattice. We found almost equal $I(p)$ on varying the lattice constants a and b of the two unit cells with constant V_c and mean orientation.[28] The small remaining difference is due to different stacking of ab layers along the c axis. These hypothetical structures illustrate that although contributions to $I(p)$ of one or a few molecules are negligible, small changes become significant collectively.

P and F are centrosymmetric molecules. As noted below Eq. (8), the leading term of $W(p) = -e\Phi^{(g)}(0)$ is then the potential at the center of the molecule. $\Phi^{(g)}(\mathbf{r})$ is a smooth function of $\mathbf{r}$ in the volume of molecule p and ionization of a π-MO mainly changes the charge density at C atoms. Figure 4 shows $\Phi^{(g)}(\mathbf{r}_m)$ at half of the atomic positions of P and F in a standing ab bilayer and a lying monolayer. The bilayer potential does not have inversion symmetry, but deviations are not apparent on this scale. The dashed lines in Fig. 4 mark $\Phi^{(g)}(0)$ in each case, whose values are given in Fig. 2. The approximation $-e\Phi^{(g)}(0)$ deviates by less than 0.06 eV from $W(p)$ in Table II. Hence $\Phi^{(g)}(0)$ is a quantitative measure of molecular electrostatics and tedious evaluation of the potential at every atom can be avoided. By contrast, $\Phi^{(g)}(0)$ cannot be used for the cross terms in Eq. (7), which represent charge redistribution in molecules and vanish in a constant potential.

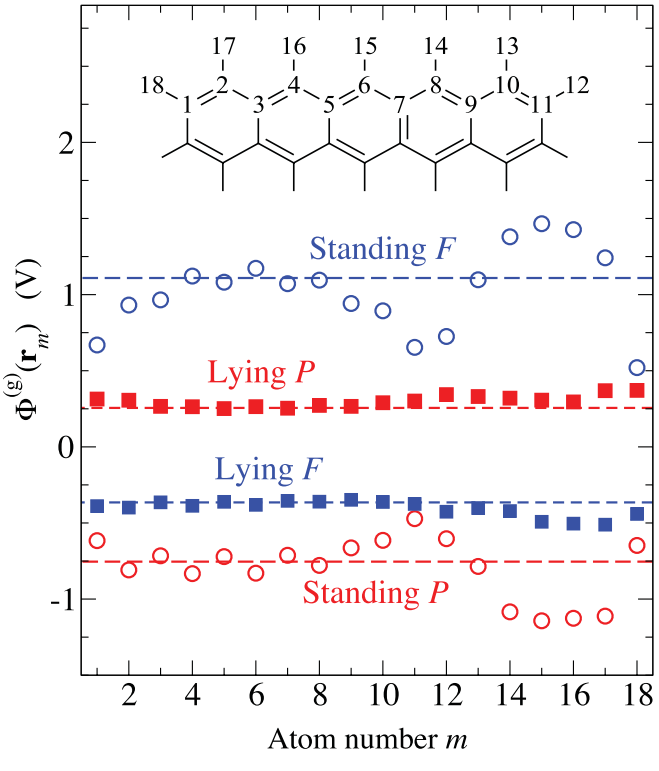

FIG. 4. (Color online) Calculated electrostatic potential $\Phi^{(g)}(\mathbf{r}_m)$ in V at the indicated atoms of extended standing bilayers or lying monolayers of pentacene (P) or perfluoropentacene (F). Dotted lines are $\Phi^{(g)}(0)$, the potential at the center of P or F.

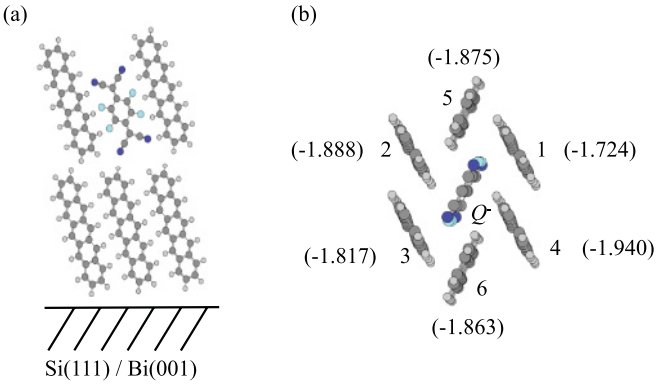

FIG. 5. (Color online) (a) Schematic representation of a $Q =$ F4TCNQ dopant in a surface cavity of a pentacene (P) bilayer. (b) Top view of the negatively charged Q^- and its Coulomb interaction $V(R)$ in eV, Eq. (12), with neighboring P^+ cations.

IV. PENTACENE FILMS WITH F4TCNQ DOPANTS

Multilayer pentacene films have standing molecules. The STM images of Ha and Kahn[8] showed a highly crystalline ab plane with a few vacancies, some of which can be filled by the strong π acceptor $Q =$ F4TCNQ as shown schematically in Fig. 5(a). Tunneling into occupied P states is greatly enhanced near Q while tunneling into unoccupied states is almost the same near and far from Q. The strong asymmetry between occupied and unoccupied states is decisive evidence[8] for Q in vacancies rather than on the surface. Ha and Kahn[8] then deposited another P layer on the doped surface and report STM images near and far from subsurface dopants. Tunneling into occupied states is suppressed (dark spot) near a subsurface Q while tunneling into unoccupied states is enhanced (bright spot)[8].

Neither surface nor subsurface Q changes the structure in any discernible way. Accordingly, we consider Q to be an electronic dopant that changes $\Phi^{(g)}(\mathbf{r})$ at nearby sites. Since F4TCNQ is a strong π acceptor, we suppose that Q^-P^+ ion pairs are formed, as expected on the basis of comparable measured[4] $A(Q)$ and $I(P)$ in thick films. Coulomb interactions favor adjacent ions by some 2 eV and ion pairs in the same ab layer and by about 0.5 eV over ions in adjacent layers. Heavier doping has recently provided evidence[36] for a charge transfer (CT) complex between Q and P, and such a complex for Q in a vacancy would also be in the same ab layer. Coulomb interactions in organic CT crystals are taken to be proportional to the ionic character.[37] Our results for Q^-P^+ correspond to the transfer of one electron.

The sharp STM tip generates strong local electric fields as is well known from field emission. The electrostatic potential of the tip could in principle be included in the present analysis, for example as a point source. However, neither the magnitude of the source nor the tip-to-surface distance h is known precisely. STM yields accurate variations of h for tunneling near and far from dopants. Accordingly, we focus on electrostatic changes due to dopants.

Van der Waals interactions of Q are maximized in Fig. 5(a) by making direct contact with P in the second ab layer. The center of Q is about 1 Å deeper than the center of P. The dipole of Q^-P^+ has a component normal to the surface that is important for our analysis. The precise location of the anion is hypothetical, but the potential depends weakly on location. The Coulomb attraction $V(R)$ between Q^- at the origin and a P^+ centered at R is evaluated using B3LYP with the 6-311^{++}G** basis

$$V(R) = {}^3E(R) - E(Q^-) - E(P^+). \tag{12}$$

Here ${}^3E(R)$ is the triplet ground state of the ion pair, which suppresses bond formation and automatically includes ion-ion polarization. The other energies are the ground states of the two ions. Figure 5(b) is a top view of Q^- in a P layer and lists $V(R)$ for the indicated neighbors. Since tilted molecules break inversion, $V(R)$ is slightly different for all neighbors when Q is in contact with the lower ab plane. We consider the cation to be localized but not static. The relative weight of an ion pair is given by the Boltzmann factor $\exp(-V(R)/k_BT)$.

STM of P near or far from Q probes how $I(p)$ or $A(p)$ changes under conditions of essentially identical contact between tip and molecules. The images show variations of the tip height h at constant current. In the present model, an electrostatic potential of a Q^-P^+ ion pair shifts $I(p)$ and $A(p)$ relative to distant P. The electrostatic energy $\Delta W(p)$ at molecule p relative to a distant P follows from Eq. (2)

$$\Delta W(p) = -\int d^3\vec{r}\,\Delta\rho_{\pm}^{(g)}(\vec{r})\Delta\Phi_p^{(g)}(\vec{r}). \tag{13}$$

Here $\Delta\Phi^{(g)}$ is the potential change due to the ion pair generated by the density $\rho(r,R)$ of ${}^3E(R)$ instead of two neutral molecules. We evaluate $\Delta\Phi^{(g)}(x,y,0)$ in the ab plane on a 1 Å grid that passes through the centers of molecules at the surface. $I(p)$ variations are estimated as $\Delta W(p) = -e\Delta\Phi^{(g)}(x,y,0)$ at $p(x,y)$. The cation may be any P in the ab layer next to Q. We also compute the average potential for a cation distributed over two or more neighbors.[28] An average potential mimics cation hopping in the ab plane on a time scale faster than scanning.

We start with an ion pair in the ab layer below the surface. Tunneling into occupied states or unoccupied states on the surface varies as $I(p)$ or $A(p) = |e|\Delta\Phi_p^{(g)}(0)$. The positive potential generates a dark spot in occupied states and a bright spot in unoccupied states. A bright spot is shown in Fig. 6 (inset) on a grid that marks the centers of P molecules on the surface and a line along which $|e|\Delta\Phi_p^{(g)}(0)$ is calculated. The potential along the line is plotted in the main figure for a bright spot and for the corresponding dark spot for tunneling into occupied states. The open symbols refer to a localized P^+ at site 4 in Fig. 5(b) with the lowest energy while the closed symbols show a Boltzmann distributed cation at 300 K over the six neighbors of Q. The observed bright spot as a function of tip height h is shown in Fig. 2 of Ref. 9, and variations $h(x)$ for subsurface dopants are shown in Fig. 6 along the same line. Tunneling depends on surface corrugation as well as $I(p)$ or $A(p)$, which are smooth functions of $\Delta\Phi_p^{(g)}$. The electrostatic potential mimics $h(x)$ and accounts for the similar shapes of bright and dark spots. We are not aware of quantitative relations between tunneling current and either tip height or local potential.

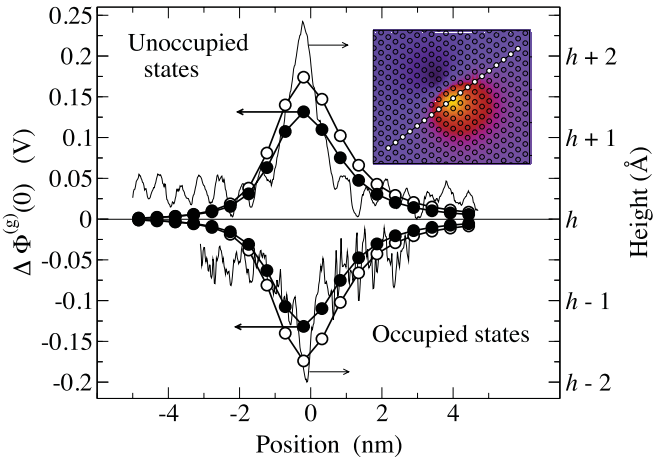

FIG. 6. (Color online) Calculated potential $\Delta\Phi_p^{(g)}(0)$ in V in the plane passing through the centers of P on the surface due to a subsurface F4TCNQ dopant. The inset shows the path. Open and closed symbols refer to $\Delta\Phi^{(g)}(0)$ at P centers for a localized hole at the lowest energy site and a Boltzmann distributed hole at 300 K. STM traces from Ref. 9 show variations of the tip height h for tunneling into unoccupied and occupied states along the same paths.

For surface dopants, we evaluate $\Delta\Phi_p^{(g)}(0)$ the same way at the centers of P at the surface. We ignore tunneling through Q since the F4TCNQ molecule is smaller and below the surface even if it is not shifted down as sketched in Fig. 5(a). We model the electric field of the tip as follows: a negative tip for tunneling into unoccupied states pins P^+ below the tip, while a positive tip for tunneling into occupied states excludes a hole below the tip. The modest energy differences between ion pairs in Fig. 5(b) make it plausible for the tip to control the ion pair's orientation. This simple idea accounts for the strong asymmetry of tunneling into occupied and unoccupied states near surface dopants.

Tunneling into occupied states is through P next to or far from Q^-, and $I(P)$ is strongly lowered next to a surface dopant by the Q^-P^+ ion pair. A bright spot is shown in Fig. 7 (inset) on a grid that marks the centers of P and a line along which $|e|\Delta\Phi_p^{(g)}(0)$ is calculated. The potential $\Delta\Phi_p^{(g)}(0)$ is plotted in the main figure. When the tip is over molecule 1 in Fig. 5(b), we assume that the hole is equally shared between molecules 2, 3, and 4. Conversely, the tip over 3 leads to a hole shared by 1, 2, and 4. Except when the tip is over a neighbor, $\Delta\Phi_p^{(g)}(0)$ is evaluated as the Boltzmann distributed cation at 300 K over all six neighbors. Multiple orientations of the ion pair generate a small potential except next to the dopant. The steep sides and increased width of $\Delta\Phi_p^{(g)}(0)$ in Fig. 7 follows directly from lower $I(P)$ next to the ion pair. The observed tip height $h(x)$

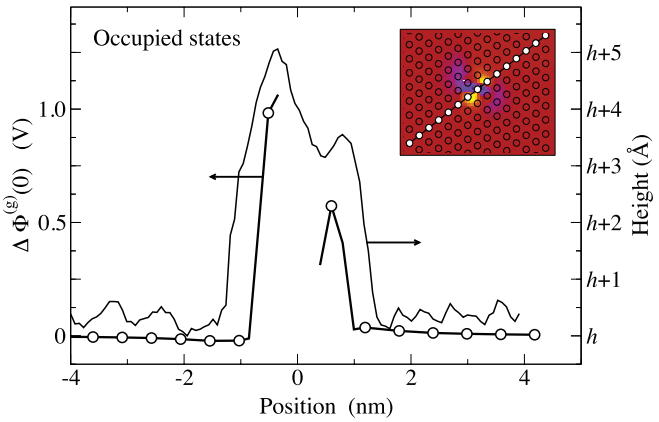

FIG. 7. (Color online) Calculated potential $\Delta\Phi_p^{(g)}(0)$ in V in the plane passing through the center of P on the surface due to a surface F4TCNQ dopant. The inset shows the path. STM traces from Ref. 38 show variations of the tip height h for tunneling into occupied states along this path.

along the same line in Fig. 7 also has steeper sides, greater width and different profile than for subsurface dopants.[38] As noted in connection with Q^-P^+, tilted molecules lead to different $\Delta\Phi_p^{(g)}(0)$ on either side of Q and this asymmetry appears in the STM image. The potential becomes negative directly over Q, thereby suppressing tunneling into occupied states quite aside from reduced tip/Q contact. The width and steep sides of bright spots for tunneling into occupied states are almost completely due to the exclusion of P^+ under the tip.

Tunneling into unoccupied states is through P^+ next to a surface dopant. The electron affinity of the cation radical is very large since in the gas phase $A_g(P^+) = I_g(P)$. Electron injection into P^+ generates PQ^-. To complete the circuit, an electron must enter an unoccupied P state with regeneration of the P^+Q^- ion pair. Tunneling into unoccupied states is via P^- states. We evaluate the potential change in Eq. (13) due to a surface dopant at the centers of P in the ab layer below the surface and find $\Delta\Phi_p^{(g)}(0) = 0.013$ V below the pinned P^+, which is an order of magnitude smaller than for subsurface dopants. Small $\Delta\Phi_p^{(g)}(0)$ is consistent with essentially no change of tunneling into unoccupied states near a surface dopant and implies almost equal $A(P)$ at P far from the Q and below the pinned P^+. To follow up, we carried out a self-consistent INDO/S calculation of the electrostatic energy $E_0(P^+P^-)$ in Eq. (3) for a P^+P^- ion pair on the surface of a film with four ab layers. The structure is more accurate with P^- replacing Q^-. We evaluate $E_0(P^+P^-p')$ for an anion at p' below the cation and find $P_-(p') = 0.95$ eV for

$$P_-(p') = E_0(P^+P^-p') - E_0(P^+P^-). \tag{14}$$

The self-consistent INDO/S polarization energy of an anion on the surface of a four-layer film of neutral P is $P_-(p) = 0.91$ eV, slightly less than $P_-(p')$, and tunneling into unoccupied states is again enhanced a bit.

Our treatment of subsurface dopants incorporates Q^-P^+ ion pairs and cation hopping suggested by Ha and Kahn.[9] They considered cations in adjacent ab layers, however, and cations in adjacent layers were crucial for their modeling of Fig. 6 in terms of a truncated Coulomb potential.[9] They did not model surface dopants. We limit ion pairs to the same ab layer on energetic grounds, evaluate the potential $\Delta\Phi_p^{(g)}(0)$ of surface or subsurface dopants, and relate tunneling changes to $I(p)$ for occupied states or of $A(p)$ for unoccupied states. The great asymmetry of tunneling into occupied and unoccupied states at surface dopants is due to cation motion induced by the tip.

V. DISCUSSION

The general treatment of ionization processes in organic thin films holds in the limit of no intermolecular overlap. As in molecular exciton theory, we rely on molecular and structural inputs. Improved quantum theory for molecular ionization potentials, electron affinities, and polarizability can immediately be incorporated, as can more accurate film structures. We have focused on the gas-phase electrostatic potential $\Phi^{(g)}(\mathbf{r})$ of neutral molecules and a few ions. Electronic polarization $E_P(p)$, the first term of Eq. (11), is treated self-consistently as before[18] and depends on molecular polarizability. Improved $E_P(p)$ is desirable but difficult. Electronic contributions to the ionization potential $I(p)$ or electron affinity $A(p)$ of molecule p in a film are found directly using Eq. (1) without adjustable parameters. No overlap is clearly a better approximation for some organic films than for others, and pentacene films may be particularly favorable systems.

In general, $I(p)$ depends on molecular orientation, on film composition and on depth from the surface. The UPS spectra of P and F films discussed in Sec. III illustrate the orientation dependence of $I(p)$. At present resolution, the approximation of no overlap is quantitative. The composition dependence is open pending structural information as shown by the range of $I(p)$ in 1:1 films in hypothetical limiting structures. Trends for either orientation or composition can be understood directly from molecular electrostatics, as emphasized by Heimel *et al.*[7] The present work supports their conclusions and places electrostatic contributions on a quantitative basis in two ways.

First, the molecular potential $\Phi^{(g)}(\mathbf{r})$ and electrostatic energy $W(p)$ in Eq. (2) are well defined and can readily be evaluated in crystalline films. Second, the potential $\Phi^{(g)}(0)$ at molecular centers is a simple quantitative measure of electrostatics. We have emphasized that both electronic polarization $E_P(p)$ and electrostatics contribute to $I(p)$ or $A(p)$ but they are not additive. Since $E_P(p)$ is always stabilizing and depends weakly on orientation or composition, however, electrostatics in general and $\Phi^{(g)}(0)$ in particular suffice for trends. Variations of $\Phi^{(g)}(0)$ rationalize the STM images in Sec. IV of surface and subsurface F4TCNQ dopants in pentacene films. The tip's role in the location of the cation next to the dopant is also an electrostatic effect.

P and F films in Sec. III have surfaces with uniform $I(p)$ that depends on molecular orientation while P films in Sec. IV have variable $I(p)$ and $A(p)$ that reflect the electrostatic potential of dopants. We previously considered[13] the dependence of $I(p)$ and $A(p)$ on film thickness up to $N = 10$ layers and on the layer of molecule p. $I(p)$ changes of 100–200 meV between the surface and the next layer may be detectable in favorable cases when electrostatics and polarization both increase with depth. UPS spectra of noble

gases are about twice as narrow and show resolved layers[39] or resolved surface and bulk features.[19,20] Noble gas atoms with spherically symmetric charge distributions have $W(p) = 0$, electronic polarization $E_P(p)$ and no broadening due to Franck-Condon relaxation. Distributed polarizability in widely used microelectrostatic methods[12,17] are also limited to $E_P(p)$ unless molecular shape and hence multipoles are explicitly considered. $W(p)$ and electrostatic potentials are a basic difference between atoms and molecules that has been neglected until recently. UPS spectra of small molecules may show resolved vibronics,[40] and such broadening has been inferred for conjugated molecules relevant to organic electronics.[41] $I(p)-A(p)$ differences between organic monolayers and thick films can be seen at present resolution.[27]

We note in conclusion that $I(p)$ or $A(p)$ can be evaluated equally well for any molecule in the film, although comparison with experiment is limited to surfaces. A major application is expected to be ionization processes at buried interfaces or inside films. Such information bears directly on organic electronics and on broader questions about charge injection, charge transfer, and tunneling. In addition to the electronic polarization emphasized in previous studies, ionization in organic thin films depend on the electrostatic potential $\Phi^{(g)}(\mathbf{r})$ and its magnitude $\Phi^{(g)}(0)$ at the center of molecules.

ACKNOWLEDGMENTS

It is a pleasure to thank M. Kumar, A. Kahn, S. Ha, and N. Koch for stimulating discussions about UPS and STM measurements. We also thank G. Heimel and S. Ha for files of experimental data. We gratefully acknowledge support for this work by the National Science Foundation under the MRSEC program (DMR-0819860).

*soos@princeton.edu

[1] S. R. Forrest and M. E. Thompson (Eds.), Organic Electronics, Chem. Rev. **107**, 923 (2007).
[2] *Organic Field-Effect Transistors*, edited by Z. Bao and L. Locklin (CRC Press, New York, 2007).
[3] J. Hwang, A. Wan, and A. Kahn, Mater. Sci. Eng. R **64**, 1 (2009).
[4] W. Chen, D. Qi, X. Gao, and A. T. S. Wee, Prog. Surf. Sci. **84**, 279 (2009).
[5] *Conjugated Polymer and Molecular Interfaces*, edited by W. R. Salaneck, K. Seki, A. Kahn, and J.-J. Pireaux (Marcel Dekker, New York, 2001).
[6] I. Saltzmann, S. Duhm, G. Heimel, M. Oehzelt, R. Kniprath, R. L. Johnson, J. P. Rabe, and N. Koch, J. Amer. Chem. Soc. **130**, 12870 (2008); S. Duhm, G. Heimel, I. Salzmann, H. Glowatzki, R. L. Johnson, A. Vollmer, J. P. Rabe, and N. Koch, Nature Mat. **7**, 326 (2008).
[7] G. Heimel, I. Saltzmann, S. Duhm, and N. Koch, Chem. Mater. **23**, 359 (2011).
[8] S. D. Ha and A. Kahn, Phys. Rev. B **80**, 195410 (2009).
[9] S. D. Ha, Y. Qi, and A. Kahn, Chem. Phys. Lett. **495**, 212 (2010).
[10] F. Gutmann and L. E. Lyons, *Organic Semiconductors* (Wiley, New York, 1967), Chap. 6.
[11] M. Pope and C. E. Swenberg, *Electronic Processes in Organic Crystals* (Clarendon, Oxford, 1982), Chap. II.
[12] E. A. Silinsh and V. Capek, *Organic Molecular Crystals: Interaction, Localization and Transport Phenomena* (AIP, New York, 1994).
[13] B. J. Topham, M. Kumar, and Z. G. Soos, Chem. Phys. Lett. **493**, 251 (2010).
[14] P. J. Bounds and R. W. Munn, Chem. Phys. **59**, 41 (1981).
[15] J. D. Jackson, *Classical Electrodynamics* (Wiley, New York, 1962), Chap. 4, p. 101.
[16] N. F. Mott and M. J. Littleton, Trans. Faraday Soc. **34**, 485 (1938).
[17] J. W. Rohleder and R. W. Munn, *Magnetism and Optics of Molecular Crystals* (Wiley, New York, 1992).
[18] E. V. Tsiper and Z. G. Soos, Phys Rev. B **64**, 195124 (2001).
[19] M. Tchaplyguine, R. R. Marinho, M. Gisselbrecht, J. Schulz, N. Mårtensson, S. L. Sorensen, A. Naves de Brito, R. Feifel, G. Öhrwall, M. Lundwall, S. Svensson, and O. Björneholm, J. Chem. Phys. **120**, 345 (2004).
[20] F. G. Amar, J. Smaby, and T. J. Preston, J. Chem. Phys. **122**, 244717 (2005).
[21] D. Fox, Chem. Phys. **17**, 273 (1979).
[22] P. J. Bounds and R. W. Munn, Chem. Phys. **44**, 103 (1979).
[23] M. C. Zerner, G. H. Loew, R. F. Kirchner, and U. T. Mueller-Westerhoff, J. Am. Chem. Soc. **102**, 589 (1980).
[24] E. V. Tsiper and Z. G. Soos, Phys Rev. B **68**, 085301 (2003).
[25] J. M. Sin, E. V. Tsiper, and Z. G. Soos, Europhys. Lett. **60**, 743 (2002).
[26] I. G. Hill, A. Kahn, Z. G. Soos, and R. A. Pascal Jr., Chem. Phys. Lett. **327**, 181 (2000).
[27] E. V. Tsiper, Z. G. Soos, W. Gao, and A. Kahn, Chem. Phys. Lett. **360**, 47 (2002).
[28] B. J. Topham, Ph.D. Thesis, Princeton University, 2012.
[29] M. J. Frisch, G. W. Trucks, H. B. Schlegel, G. E. Scuseria, M. A. Robb, J. R. Cheeseman, J. A. Montgomery Jr., T. Vreven, K. N. Kudin, J. C. Burant, J. M. Millam, S. S. Iyengar, J. Tomasi, V. Barone, B. Mennucci, M. Cossi, G. Scalmani, N. Rega, G. A. Petersson, H. Nakatsuji, M. Hada, M. Ehara, K. Toyota, R. Fukuda, J. Hasegawa, M. Ishida, T. Nakajima, Y. Honda, O. Kitao, H. Nakai, M. Klene, X. Li, J. E. Knox, H. P. Hratchian, J. B. Cross, V. Bakken, C. Adamo, J. Jaramillo, R. Gomperts, R. E. Stratmann, O. Yazyev, A. J. Austin, R. Cammi, C. Pomelli, J. W. Ochterski, P. Y. Ayala, K. Morokuma, G. A. Voth, P. Salvador, J. J. Dannenberg, V. G. Zakrzewski, S. Dapprich, A. D. Daniels, M. C. Strain, O. Farkas, D. K. Malick, A. D. Rabuck, K. Raghavachari, J. B. Foresman, J. V. Ortiz, Q. Cui, A. G. Baboul, S. Clifford, J. Cioslowski, B. B. Stefanov, G. Liu, A. Liashenko, P. Piskorz, I. Komaromi, R. L. Martin, D. J. Fox, T. Keith, M. A. Al-Laham, C. Y. Peng, A. Nanayakkara, M. Challacombe, P. M. W. Gill, B. Johnson, W. Chen, M. W. Wong, C. Gonzalez, and J. A. Pople, GAUSSIAN 03, Revision C.02, (Gaussian, Inc., Wallingford, CT, 2004).
[30] N. Koch, A. Vollmer, S. Duhm, Y. Sakamoto, and T. Suzuki, Adv. Mater. **19**, 112 (2007).

[31] V. Coropceanu, M. Malagoli, D. A. da Silva Filho, N. E. Gruhn, T. G. Bill, and J. L. Brédas, Phys. Rev. Lett. **89**, 275503 (2002).
[32] M. C. R. Delgado, K. R. Pigg, D. A. da Silva Filho, N. E. Gruhn, Y. Sakamoto, T. Suzuki, R. M. Osuna, J. Casado, V. Hernández, J. T. L. Navarrete, N. G. Martinelli, J. Cornil, R. S. Sanchez-Carrera, V. Coropceanu, and J. L. Brédas, J. Amer. Chem. Soc. **131**, 1502 (2009).
[33] R. B. Campbell, J. M. Robertson, and J. Trotter, Acta Crystallogr. **15**, 289 (1962).
[34] Y. Sakamoto, T. Suzuki, M. Kobayashi, Y. Gao, Y. Fukai, Y. Inoue, F. Sato, and S. Tokito, J. Amer. Chem. **126**, 8138 (2004).
[35] S. L. Wong, H. Huang, Y. L. Huang, Y. Z. Wang, X. Y. Gao, T. Suzuki, W. Chen, and A. T. S. Wee, J. Phys. Chem. C **114**, 9356 (2010).
[36] I. Salzmann, G. Heimel, S. Duhm, M. Oehzelt, P. Pingel, R. Blum, A. Vollmer, and N. Koch (unpublished).
[37] Z. G. Soos, Annu. Rev. Phys. Chem. **25**, 121 (1974).
[38] S. D. Ha, Ph.D. Thesis, Princeton University, 2011.
[39] T. C. Chiang, G. Kaindl, and T. Mandel, Phys. Rev. B **33**, 695 (1986).
[40] T. D. Thomas, L. J. Saethre, S. L. Sorensen, and S. Swensson, J. Chem. Phys. **109**, 1041 (1998).
[41] S. Kera, H. Yamane, and N. Ueno, Progr. Surf. Sci. **84**, 135 (2009).